ELSEVIER

Earth and Planetary Science Letters 201 (2002) 509–523

EPSL

www.elsevier.com/locate/epsl

Limitations on stratigraphic analyses due to incomplete age control and their relevance to sedimentary paleomagnetism

D.G. McMillan *, C.G. Constable, R.L. Parker

Institute of Geophysics and Planetary Physics, Scripps Institution of Oceanography, La Jolla, CA 92093-0225, USA

Received 28 January 2002; received in revised form 28 May 2002; accepted 1 June 2002

Abstract

A major limitation in the analysis of physical quantities measured from a stratigraphic core is incomplete knowledge of the depth to age relationship for the core. Records derived from diverse locations are often compared or combined to construct records that represent a global signal. Time series analysis of individual or combined records is commonly employed to seek quasi-periodic components or characterize the timescales of relevant physical processes. Assumptions that are frequently made in the approximation of depth to age relationships can have a dramatic and harmful effect on the spectral content of records from stratigraphic cores. A common procedure for estimating ages in a set of samples from a stratigraphic core is to assign, based on complementary data, the ages at a number of depths (tie points) and then assume a uniform accumulation rate between the tie points. Imprecisely dated or misidentified tie points and naturally varying accumulation rates give rise to discrepancies between the inferred and the actual ages of a sample. We develop a statistical model for age uncertainties in stratigraphic cores that treats the true, but in practice unknown, ages of core samples as random variables. For inaccuracies in the ages of tie points, we draw the error from a zero-mean normal distribution. For a variable accumulation rate, we require the actual ages of a sequence of samples to be monotonically increasing and the age errors to have the form of a Brownian bridge. That is, the errors are zero at the tie points. The actual ages are modeled by integrating a piecewise constant, randomly varying accumulation rate. In each case, our analysis yields closed form expressions for the expected value and variance of resulting errors in age at any depth in the core. By Monte Carlo simulation with plausible parameters, we find that age errors across a paleomagnetic record due to misdated tie points are likely of the same order as the tie point discrepancies. Those due to accumulation rate variations can be as large as 30 kyr, but are probably less than 10 kyr. We provide a method by which error estimates like these can be made for similar stratigraphic dating problems and apply our statistical model to an idealized marine sedimentary paleomagnetic record. Both types of errors severely degrade the spectral content of the inferred record. We quantify these effects using realistic tie point ages, their uncertainties and depositional parameters.

Keywords: chronostratigraphy; age; errors; paleomagnetism; spectral analysis

1. Introduction

Many Earth science disciplines have benefited from the coring of sediments and ice. Analysis of measurements from the cores has permitted an unprecedented view of past physical condi-

* Corresponding author. Tel.: +1-858-822-1560; Fax: +1-858-534-5332.

E-mail addresses: dmcmillan@ucsd.edu (D.G. McMillan), cconstable@ucsd.edu (C.G. Constable), rlparker@ucsd.edu (R.L. Parker).

0012-821X/02/$ – see front matter
PII: S0012-821X(02)00747-1

tions, often to ages of hundreds of thousands and even millions of years. From these cores, measurements of oxygen isotopes [1–3], cosmogenic isotopes [4–7], and physical quantities, such as electrical conductivity [8–10] and magnetic properties [11,12], yield information about a variety of Earth systems including the atmosphere and oceans, climate and dynamics of the deep interior. The preeminent limitation in making worthwhile observations about these systems is the ability to assign sufficiently accurate ages to measurements made from sediment and ice cores.

A reliable method of assigning relative dates to core samples is by layer counting. In ice cores and some sedimentary environments, annual variations in accumulation, content, or texture are easily identified and counted [13,14]. Problems in estimating a depth–age relationship arise when ice layers are disrupted by flow [15,16] or become more difficult to identify when overburden pressure and temperature increases cause recrystallization of the ice deep in a glacier [17,18]. In sedimentary environments, hydrological or biological disturbances are possible and errors in counting can occur in sections of the core where an unconformity or disturbance is identified [19], or where an erosional event is not identified [20]. Radiometric dating provides an alternative, but has its shortcomings. ^{14}C dating is only useful to about 40 or 50 kyr in age. In addition, there is a significant and not fully understood discrepancy between radiocarbon dates and those found by the counting of tree rings and by other radiometric methods [21,22]. Recent advances in uranium–thorium dating provide an excellent alternative to ^{14}C that has a practical range to about 500 kyr [23]. The method has been used to date corals but not widely applied to marine sediments. Dating methods that are less accurate but popular in many stratigraphic contexts, especially for records that exceed 100 kyr, involve the identification of specific events, such as fossil taxon-range ends [24], ash layers [25], climate signals [12] or geomagnetic reversals [26], in the record and the assignment of their ages based on other geophysical data.

We address the inaccuracies that result from dating core samples by interpolation between pairs of control points (herein referred to as tie points) that have ages from a complementary source assigned to them. The inaccuracies exist due to uncertainties in the ages of the tie points and assumptions about the variations in accumulation rates between the tie points. In the study of ice cores, when counting of seasonal layers becomes difficult, ages can be assigned through flow modeling. This is accomplished by specifying an accumulation rate and integrating a layer thickness function between pairs of tie points [27]. It is equivalent to interpolation of ages by some, possibly non-linear, function (see [28] for a recent example). Differences between the actual accumulation history and the specified one give rise to inaccuracies in the depth–age relationship. In oceanographic depth profiling, Moore and Thompson [29] examine the effects of 'jittered sampling' on the spectral character of the signal being sampled. They define jitter as the effect of unevenly spaced samples that have been assumed evenly spaced. Using a statistical formalism, Moore and Thompson calculate analytically the disturbance of simple spectral densities caused by Gaussian jitter. However, they allow for the interchange of their samples, a phenomenon that is generally unlikely in stratigraphic problems. Jitter is defined more rigorously by Huybers and Wunsch [30] in the stratigraphic context. They establish a $\delta^{18}O$ chronology from marine sediments independent of orbital tuning and based on the assumption of uniform accumulation between tie points. The authors acknowledge the uncertainties that arise by random variations in accumulation rates and propose a definition of jitter based on a stochastic component of accumulation rate. Agrinier et al. [31] provide a different approach to a similar problem: the estimation of ages of geomagnetic reversals recorded by sea floor anomalies, where the unknown accumulation rate is plate velocity. Their statistical analyses yield a numerical method whereby different polarity timescales and their likelihoods are computed given two end-member plate velocity functions.

In sedimentary paleomagnetism, it has become commonplace to combine records that span thousands to millions of years. Multiple records from one locality are combined with the intention of

increasing the signal of regional secular variation over the noise of recording and measurement processes (for example, [32]). Those from geographically diverse locations are combined to eliminate local and short period variations, revealing signals that reflect global secular variation [12,33]. In both cases, spectral analysis has been used to establish characteristic timescales of secular variations in Earth's core field that are thought to reflect geodynamo processes (for example, [34]). However, because depth to age relationships in sedimentary cores are poorly known and may vary significantly over small geographic distances, spectral comparisons and composite paleomagnetic records should be approached with caution.

The depth to age relationship in marine sediments is usually based on the identification of key changes in oxygen isotope ($\delta^{18}O$) records from the paleomagnetic cores and their comparison with an established $\delta^{18}O$ chronology [1,35]. Nearby cores are often dated relative to one with a $\delta^{18}O$ chronology by correlating geological features in the core, such as volcanic ash layers [36], or by correlating identifiable features in a related record, such as magnetic susceptibility [37] or light reflectance [38]. For a particular core, the result is a finite number of tie point ages assigned to a corresponding set of down-core depths. It is then customary to assume that the accumulation rate is constant between each pair of tie points, rendering a piecewise linear relationship between depth and age.

In general, tie points are imprecisely dated, or may even be improperly identified, and there are natural variations in accumulation rates that limit the accuracy of the age assigned to a particular core measurement. The difference between the actual age and inferred age of a sample we call the age error. We refer to age errors due to uncertain tie point dates as event errors, and those due to variable accumulation rates as interpolation errors.

To estimate the magnitudes of these errors, we develop a statistical framework based on traditional analysis of dating uncertainty and a stochastic model representing variations in a physical process. We assume point samples that represent an instantaneous recording of the magnetic field and treat as random variables (RVs) the actual, but in practice unknown, ages of the samples. Tie point ages derived from isotopic, radiometric and geologic sources have uncertainties associated with them. We model these errors as independent, zero-mean normal RVs with standard deviations that are equal to the uncertainties of the estimated ages. Accumulation rates vary both deterministically and stochastically, with the former being driven primarily by climatic forcing. Here we focus on the stochastic, independent accumulation rate variations that occur between times of adjacent samples. We seek a simple model that generates constrained perturbations to inferred ages, without altering their order, that are a result of physically plausible perturbations in accumulation rate. To this end, we formulate a Brownian bridge [39] model of the actual ages of paleomagnetic measurements and derive age error expressions that include contributions from both event and interpolation errors. We give expressions for their means and variances and approximations for the mean and variance of the accumulation rate perturbation. A method of applying our analysis to stratigraphic data is presented. Last, we examine the effects of particular realizations of these errors, individually and in combination, on the spectral content of idealized paleomagnetic records.

2. Event errors

In this section, we ignore variations in accumulation rate and examine the effects of uncertain tie point ages on the age errors between two tie points. Consider the case in which we have two tie points at depths z_0 and z_M and their inferred ages are t_0 and t_M (see Table 2 for a list of symbols). Based on a constant accumulation rate, the inferred age at any depth $z_0 \leq z \leq z_M$ is:

$$t(z) = t_0 + \frac{z - z_0}{z_M - z_0}(t_M - t_0) \quad (1)$$

The quantity $(z-z_0)/(z_M-z_0)$ is the fractional distance between tie points and we abbreviate it with α. If the inferred accumulation rate is not constant, we replace Eq. 1 with the appropriate ex-

pression and follow the same procedure to derive an expression for the event error. Let the actual ages of the tie points be τ_0 and τ_M. Then, following Eq. 1, the event error for each sample is:

$$\varepsilon(z) = \tau(z) - t(z) =$$

$$\tau_0 + \alpha(\tau_M - \tau_0) - [t_0 + \alpha(t_M - t_0)] \quad (2)$$

After a little rearrangement, Eq. 2 becomes:

$$\varepsilon(z) = \varepsilon_0(1-\alpha) + \varepsilon_M\alpha \quad (3)$$

where $\varepsilon_0 = \tau_0 - t_0$ and $\varepsilon_M = \tau_M - t_M$ are the errors in the tie point ages. This expression gives the event error for different values of ε_0 and ε_M. The event error can be as large as either tie point error, but is always less than or equal to the larger of the two. In addition, the contribution of each tie point error to the total event error is weighted by the sample's distance from each tie point.

We calculate statistical properties of several quantities, such as age errors, based on the following definitions. The expected value of a RV Y with probability distribution function $f(y)$ is:

$$\mathrm{E}[Y] = \int_{-\infty}^{\infty} y f(y)\, \mathrm{d}y$$

and its variance is:

$$\mathrm{VAR}[Y] = \mathrm{E}[(Y - \mathrm{E}[Y])^2]$$

We now model the tie point age errors as independent, zero-mean normal RVs with variances of σ_0^2 and σ_M^2. In practice, we choose the variances to be those corresponding to the age estimates t_0 and t_M. Then the expected value of Eq. 3 is:

$$\mathrm{E}[\varepsilon] = 0 \quad (4)$$

for $z_0 \le z \le z_M$. Further, the variance of the event error is given by:

$$\mathrm{VAR}[\varepsilon] = \sigma_0^2(1-\alpha)^2 + \sigma_M^2\alpha^2 \quad (5)$$

We note the similarity to Eq. 3; the variance of the event error is a sum of the squared uncertainties in the tie points weighted by the squared distance from the tie points.

3. Interpolation errors

3.1. Random accumulation rate variations

We now turn to the case in which we assume the ages of two tie points are known exactly and examine the effects of a variable accumulation rate on the ages of core samples between the tie points. The tie points are at depths z_0 and z_M and their ages τ_0 and τ_M are presumed to be known exactly. We seek a simple statistical model that produces random errors in the ages of the samples through variations in accumulation rate. Since the ages are constrained by the tie points at each end of the interval, we choose a good neutral model for the errors in the form of a Brownian bridge ([39] and see also [40] for an application to geomagnetism), in which the errors at the end points are zero and vary randomly in between. Our model consists of two parts. The first yields a discrete set of random steps in accumulation rate at evenly spaced depths. The second provides a way to estimate the actual age, and age error, at any depth between the tie points.

We begin with a sequence of independent, identically distributed RVs designated X_i, $i = 1, 2, \ldots, M$, which are uniformly distributed on the interval $[1-a, 1+a]$. The distribution has a width of $2a$, where $0 < a \le 1$. We take the partial sum:

$$r_k = \frac{L}{s}\sum_{i=1}^{k} X_i, \quad k = 1, 2, \ldots, M \quad (6)$$

where $\bar{s} = (z_M - z_0)/(t_M - t_0)$ is the inferred constant accumulation rate, or background rate. Let $r_0 = 0$. The sequence of ages r_k, $k = 0, 1, 2, \ldots, M$ is monotonically increasing and, on average, spans a time interval $ML/\bar{s}$ or, equivalently, $t_M - t_0$. The size of L describes the lengthscale over which accumulation rates vary, while the size of a controls the magnitudes of these variations through the minimum and maximum allowable distances between adjacent elements of the sum. The following are statistical properties of the

sum in Eq. 6:

$$\mathrm{E}[r_k] = k\frac{L}{\bar{s}}, \quad k = 0,\ 1,\ ...,\ M \tag{7}$$

$$\mathrm{VAR}[r_k] = \frac{a^2}{3}k\left(\frac{L}{\bar{s}}\right)^2, \quad k = 0,\ 1,\ ...,\ M \tag{8}$$

We transform the sequence r_k to find the ages of the accumulation rate jumps according to the 'modified Brownian bridge':

$$\tau_k = (\tau_M - \tau_0 - r_M)\frac{k}{M} + r_k + \tau_0, \quad k = 1,\ 2,\ ...,\ M-1 \tag{9}$$

which stretches and/or shrinks the sequence to fit in the interval $[\tau_0,\ \tau_M]$ and clamps the end points.

Then, the piecewise constant accumulation rate is:

$$s_k = \frac{L}{\Delta\tau_k}, \quad k = 1, ..., M \tag{10}$$

where $\Delta\tau_k = \tau_k - \tau_{k-1}$. According to Eq. 10, small values of $\Delta\tau_k$ correspond to large accumulation rates (Fig. 1). Since the transformation given by Eq. 9 does not maintain the size of $\Delta\tau_k$ with respect to the spacing of r_k, it is possible that the transformed sequence is not monotonically increasing, in which case $\Delta\tau_k < 0$ for at least one value of k. Moderating the distribution width parameter a alleviates these two potential problems. We briefly describe the effects of the choice of a on accumulation rate variations and, in Section 3.3, the monotonicity of τ_k.

We define the relative perturbation in accumulation rate as:

$$s_k^* = \frac{s_k - \bar{s}}{\bar{s}}, \quad k = 1, ..., M \tag{11}$$

The relative perturbation is a RV, but is a nonlinear function of τ_k. The expression is linearized by expanding in a first order Taylor series about $\mathrm{E}[\Delta\tau_k]$ [41]. This yields the following approximations:

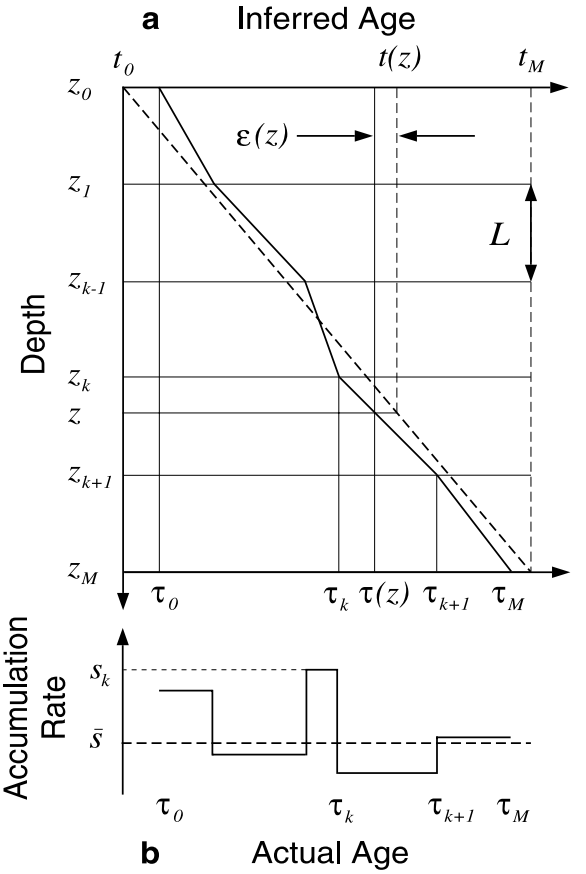

Fig. 1. Determining ages and accumulation rates. (a) The difference in the actual (solid) and inferred depth–age relationships introduces an age error $\varepsilon(z) = \tau(z) - t(z)$ at sample depth z. (b) The stochastically varying accumulation rate s_k (solid) and the inferred constant rate $\bar{s}$ from our statistical model.

$$\mathrm{E}[s_k^*] \approx \frac{a^2}{3}\left(1 - \frac{1}{M}\right), \quad k = 1, ..., M \tag{12}$$

$$\mathrm{VAR}[s_k^*] \approx \frac{a^2}{3}\left(1 - \frac{1}{M}\right), \quad k = 1, ..., M \tag{13}$$

These approximations are good when a is less than 1/3. In this range of a, s_k^* may be approximated by a uniform distribution on the interval $[-a,\ a(1+2a/3)]$. As a becomes larger the distribution of s_k^* tends to grow a longer tail on the positive side, while the size of a directly controls the probable size of s_k^*, as shown in Fig. 2.

3.2. The Brownian bridge model for age errors

We now derive an expression for the age error at a core depth z due to the randomly varying accumulation rate described above. The actual age at z is found by integrating the reciprocal accumulation rate $1/s_k$ with respect to depth. The result is:

$$\tau(z) = \tau_k + \frac{z-z_k}{L}\Delta\tau_{k+1} \tag{14}$$

for $z_k \le z < z_{k+1}$ and $k = 0, 1, 2, \ldots, M-1$. The quantity $(z-z_k)/L$ is the fractional distance between successive jumps in accumulation rate and we abbreviate it with β.

Following Eq. 1 for the inferred ages of the samples based on a constant accumulation rate, the interpolation error for each sample is:

$$\varepsilon(z) = \tau(z) - t(z) =$$

$$\tau_k + \beta\Delta\tau_{k+1} - [t_0 + \alpha(t_M - t_0)] \tag{15}$$

But by hypothesis the errors are zero at the end points, so $\tau_0 = t_0$ and $\tau_M = t_M$. After substituting and simplifying, we find:

$$\varepsilon(z) = \tau_k(1-\beta) + \tau_{k+1}\beta - [\tau_0(1-\alpha) + \tau_M\alpha] \tag{16}$$

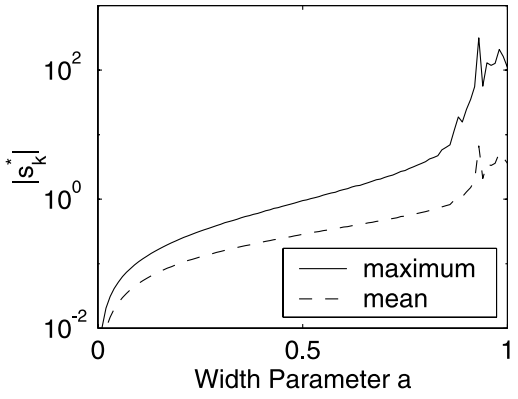

Fig. 2. Accumulation rate perturbations. The variations of the maximum (solid) and mean relative perturbation s_k^* as functions of the uniform distribution width parameter a. These relationships hold for all $\bar{s}$ and L. The oscillations above $a = 0.8$ are a random artifact due to increasing variability of s_k^* and high probability of negative $\Delta\tau_k$.

Since $\varepsilon(z_0) = \varepsilon(z_M) = 0$, the error expression has the form of a Brownian bridge, as required. The expected value of Eq. 16 is:

$$\mathrm{E}[\varepsilon] = 0 \tag{17}$$

for $z_0 \le z \le z_M$. Further, we find the variance of the interpolation error is given by:

$$\mathrm{VAR}[\varepsilon] =$$

$$\left(\frac{L}{\bar{s}}\right)^2\frac{a^2}{3}\left[k\left(1-\frac{k}{M}\right) - 2\beta\frac{k}{M} + \beta^2\left(1-\frac{1}{M}\right)\right] \tag{18}$$

for $z_k \le z < z_{k+1}$ and $k = 0, 1, \ldots, M-1$.

3.3. Practical details

For marine sediments, a $\delta^{18}O$ database such as SPECMAP [2], comprises a set of cores and, for each core, age estimates of 20 to 50 tie points over the last few hundred thousand years. Examination of the database reveals that accumulation rate variations can range from 50 to 100% over long and short time-scales and that variations of this size occur frequently and are common in globally distributed cores during climatically stable epochs (i.e. glacial and interglacial). To achieve $s_k^* \sim \mathcal{O}(1)$ (on the order of magnitude of 1) as suggested by SPECMAP data, we choose a around 0.5 (Fig. 2). However, to compare our statistical model to observation, we require a more precise depth–age relation between two tie points that are separated by $\mathcal{O}(10)$ kyr. To this end, we use the radiometrically dated section of core P094 [42] that spans about 1–20 kyr in age and comprises 12 distinct age estimates. We assume that these age determinations and those of the two surrounding tie points are exact. The measured and modeled accumulation rate variations and their histograms (Fig. 3) indicate this realization represents a physically plausible process.

Fig. 4 shows the maximum and mean magnitude of interpolation errors and their variations with a and L. The magnitudes of the errors also depend on the background accumulation rate $\bar{s}$ which is determined by the inferred ages of the tie points and their depths. For these results, we

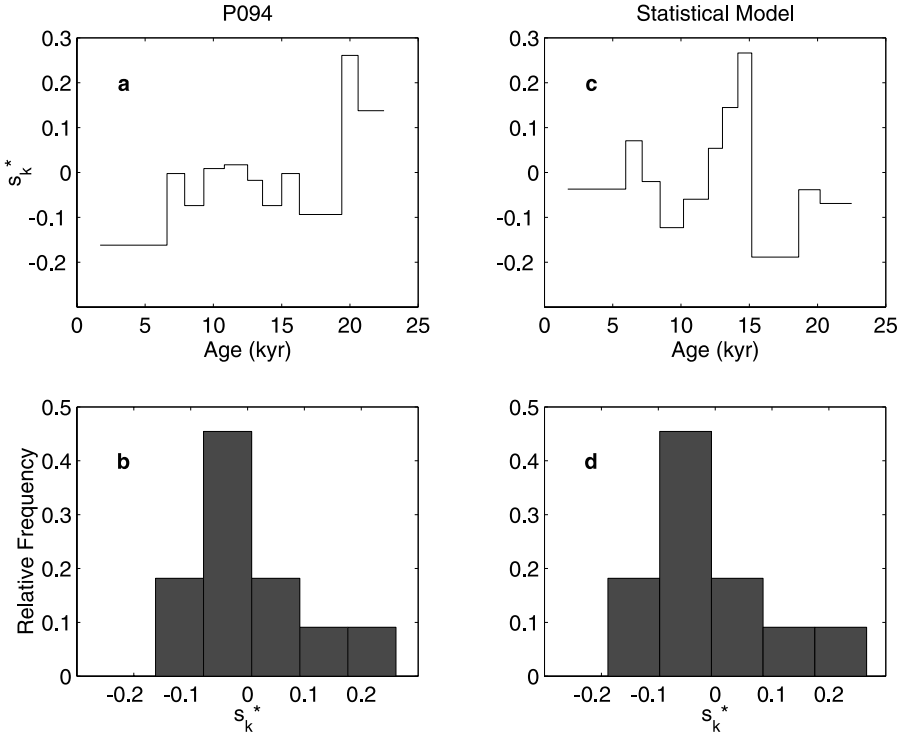

Fig. 3. Accumulation rate perturbations. Example from [42]. (a) Relative perturbation $s_k^* = (s_k - \bar{s})/\bar{s}$ with an arithmetic mean rate of $\bar{s} = 18.5$ cm kyr^{-1}. (b) Estimate of probability density function (PDF) for data in a. Example from statistical model with $a = 0.5$ and $L = 5$ cm. (c) Relative perturbation. (d) Estimate of PDF for data in c.

have used the parameters of the first segment in the record of Yamazaki and Ioka [37], for which $\bar{s} = 3.38$ cm kyr^{-1}. Since L is the lengthscale of the accumulation rate variations, doubling $\bar{s}$ is equivalent to halving L in this context (see Eq. 18). Thus, larger mean accumulation rates (smaller L) yield smaller age errors.

A negative value of $\Delta\tau_k$ is equivalent to reversing the order of two adjacent samples. Folding due to flow in ice and bioturbation or current generated overturn in sediments may produce a similar situation physically, but the details of these processes are presently beyond the scope of our model. To avoid inconsistencies, we demand that $\Delta\tau_k > 0$. It can be shown that τ_k is guaranteed to be monotonically increasing when $a \leq 1/3$. However, in practice, it is quite improbable that $\Delta\tau_k < 0$ for any k, even for larger values of a. For reasonable values of $L/\bar{s}$, the probability of this occurring is < 0.1 when $a = 0.9$ and < 0.5 when $a = 1.0$. Thus for $a \approx 0.5$, it is very unlikely that a particular realization of $\Delta\tau_k < 0$ for any k.

4. Event and interpolation errors combined

To obtain an error expression, its expected value and variance when we consider both types of age error, we begin with Eq. 15:

$$\varepsilon(z) = \tau_k + \beta\Delta\tau_{k+1} - [t_0 + \alpha(t_M - t_0)] \qquad (19)$$

Since ages t_0 and t_M are again uncertain, we cannot replace them with the actual ages τ_0 and τ_M as we did in Section 3.2. Thus, Eq. 19 is the expression we seek for the combined errors. It can be shown that this expression is the sum of the two individual errors Eqs. 3 and 16. It follows that the expected value of Eq. 19 is zero. Since the RVs in each age error case are independent and each con-

tribution has an expected value of zero, the variance of the combined errors is the sum of the two individual variances given by Eqs. 5 and 18:

$$\mathrm{VAR}[\varepsilon] = \sigma_0^2(1-\alpha)^2 + \sigma_M^2\alpha^2 + \left(\frac{L}{\bar{s}}\right)^2\frac{a^2}{3}\left[k\left(1-\frac{k}{M}\right)-2\beta\frac{k}{M}+\beta^2\left(1-\frac{1}{M}\right)\right] \quad (20)$$

Following the Taylor series method of Section 3.1, we find similar approximations for the relative accumulation rate perturbation:

$$\mathrm{E}[s_k^*] \approx \frac{\sigma_0^2+\sigma_M^2}{(t_M-t_0)^2}+\frac{a^2}{3}\left(1-\frac{1}{M}\right), \quad k=1,\ 2,\ldots,\ M \quad (21)$$

$$\mathrm{VAR}[s_k^*] \approx \frac{\sigma_0^2+\sigma_M^2}{(t_M-t_0)^2}+\frac{a^2}{3}\left(1-\frac{1}{M}\right), \quad k=1,\ldots,\ M \quad (22)$$

These expressions reflect the contributions of the tie point age errors and the variable accumulation rate. The significance of the former depends on the size of the combination of variances relative to the record length in kyr squared, or a measure of relative stretching or shrinking of the record length due to erroneous tie point ages.

5. Application to data

We briefly illustrate the application of our model to the $\delta^{18}O$ dated record of [37]. The first segment is bounded by events 2.20 and 4.24, which have dates and uncertainties of 17.85 ± 1.37 ka and 70.82 ± 3.95 ka [35]. Referring to Eq. 3, we see that in this segment the event error contribution could be as high as 3.95 kyr near 70 ka. The mean event error magnitude between two tie points is simply the average of the two uncertainties, or about 2.66 kyr for this segment. The length of the segment is approximately 180 cm, yielding $\bar{s} = 3.4$ cm kyr^{-1}. If we take a sampling interval of 2 cm and assume accumulation rate perturbations that are $\mathcal{O}(1)$ ($a = 0.5$), then, from Fig. 4a we can expect mean interpolation error

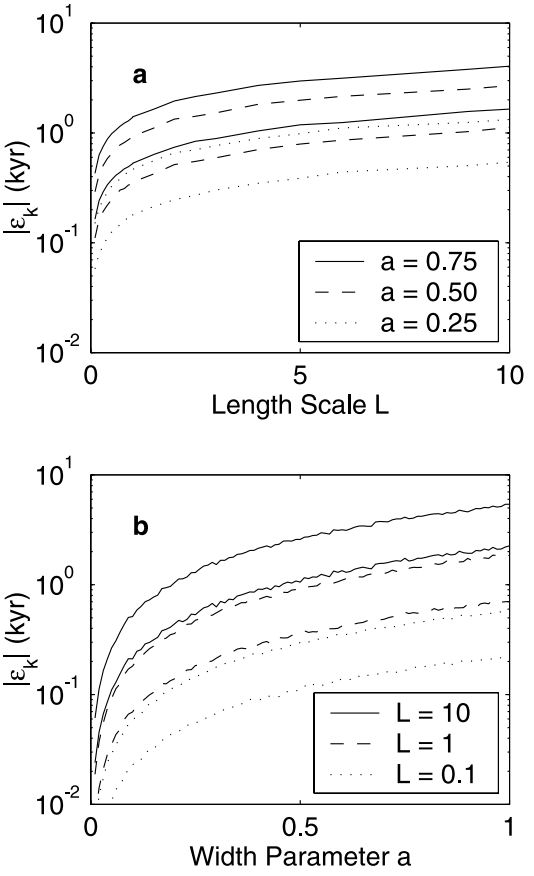

Fig. 4. Interpolation errors. (a) The maximum and mean interpolation error magnitude $|\varepsilon_k|$ as functions of a for different lengthscales $L = 0.1$, 1 and 10 cm. (b) The maximum and mean interpolation error magnitude $|\varepsilon_k|$ as functions of L for different width parameters $a = 0.25$, 0.5 and 0.75. For these examples we used $\bar{s} = 3.38$ cm kyr^{-1}, the same value as the first segment of the Yamazaki and Ioka record [37].

magnitudes that are no more than 10 kyr and maximum interpolation errors that are less than 30 kyr when the lengthscale $L = 10$ cm (or an equivalent timescale of about $L/\bar{s} = 3$ kyr). The maximum errors are quite a bit larger than the event errors. For smaller L the age errors decrease and are less than a kyr for $L < 1$ cm. The dominance of one of the two errors sources depends on the lengthscale of the accumulation rate variations.

6. Numerical experiments

We turn to paleomagnetism and apply our statistical model to a simulated magnetic intensity record generated directly from the Gauss coefficients of the uniform heat flux dynamo simulation of Glatzmaier et al. [43]. The statistical properties of the dynamo model and its relevance to the geomagnetic field are discussed by McMillan et al. [44]. Our primary assumption is: the simulation provides intensity records that are sufficiently similar to actual data to be meaningful in this context. Moreover, in treating exact intensity values, we assess the effects of event and interpolation errors in the absence of signal smoothing due depositional effects or finite sample size (see [45] for a discussion on the effects of sampling and lock-in processes). Each of our experiments involves a comparison of the spectral content of two records. The reference record is the one computed directly from the dynamo simulation and is therefore considered exact, while the second record is contaminated with age errors modeled by the above stochastic processes. The errors are found by generating random numbers and transforming them according to Eqs. 3 and 16. We compute the coherence between the two records to estimate which spectral components are retained or lost due to the age errors. In each case, we show typical results from a single realization of the randomly generated errors.

The coherence is a measure of the correlation, or linear relation, between two records at each frequency of their spectral estimates and is normalized by the root of the product of the two power spectra. As such, a high coherence does not necessarily imply that either record contains a strong signal in a particular frequency band relative to those at other frequencies. On the other hand, a high coherence implies correlation between the two records, giving a potential means to distinguish geomagnetic signals in the corrupted record. A statistical confidence level, below which the two records are likely uncorrelated, is often used to decide which values of coherence are 'high'. Two random signals produce coherence values below the P% confidence level P% of the time. In other words, random signals may show

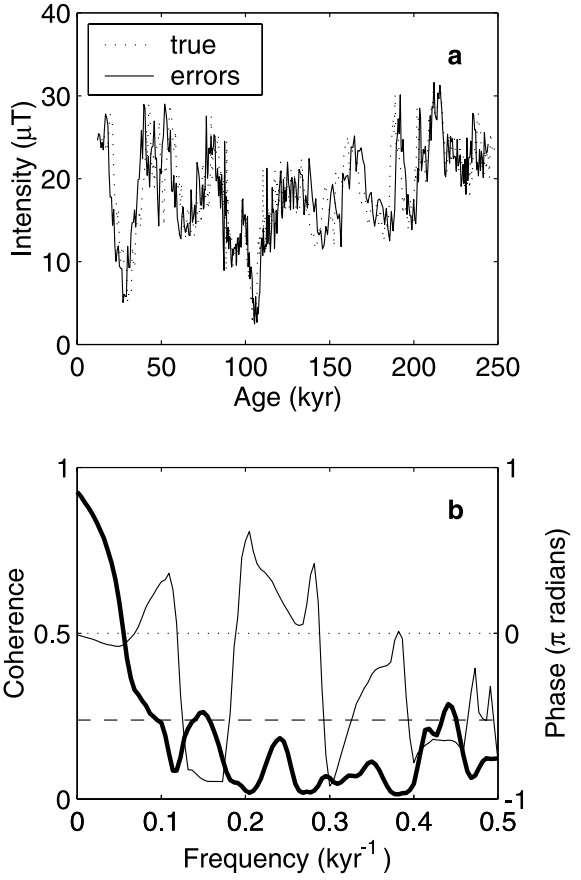

Fig. 5. Event Errors. (a) Magnetic field intensity as a function of actual age (dotted) and as a function of inferred age. (b) Coherence (thick line) and phase between the two records in (a). The dashed line is the 95% confidence level for the coherence, below which the two records are likely uncorrelated.

significant coherence at a particular frequency $(100-P)$% of the time by chance. For an alternative view, suppose we suggest the following model. The contaminated record can be computed from the clean one through a linear transfer function. Then the coherence indicates the amount of variance in the power spectrum of the contaminated record that can be explained by our model. In this case, we decide what values of coherence are 'high' based on how well we want our model to perform. For example, we might be suspicious of a coherence peak that reaches 0.4, if it is well above our chosen significance level because our model is explaining only 40% of the variance in the power spectrum of the contaminated record.

The records may not, in fact, be linearly related and our model is then incapable of explaining a certain amount of variance. For our error model, only the case of a rigid shifting of the contaminated record (both tie point ages in error by the same amount) yields a strictly linear relation between it and the original. In the following experiments, we investigate the degree to which age errors cause a violation of this linear model.

We examine the situation in which we have estimates for the ages of five tie points spanning about 230 kyr: those for oxygen isotope events 2.0, 5.0, 6.0, 7.0 and 8.0. These tie points have been chosen based on the work of Yamazaki and Ioka [37], wherein they inferred dates for five sedimentary paleomagnetic records of a similar length to ours using similar tie points. The dates and uncertainties of each of our tie points are from [35] and are listed in Table 1. We appeal to the SPECMAP database for background accumulation rates. The core V27-116 has age estimates for these tie points with few additional age estimates and relatively small accumulation rate variations between the stage boundaries (the largest is about 25%). We take a weighted average and set our background rates to $\bar{s}=3.0$, 5.6, 2.0 and 3.5 cm kyr^{-1}. We examine results for $L=1$ and 10 cm, corresponding to accumulation rate variations that occur over times of a few hundred years or a few thousand years, respectively. The maximum variations are set at approximately the same order as the background rates with $a=0.5$. We choose a depth sampling interval of 2 cm.

6.1. Event errors

Our first experiment involves modeling the errors in the tie point ages of Table 1 as stochastic processes. The error realizations are also listed in Table 1. Plots of the magnetic field intensity as functions of the actual and inferred ages are presented in Fig. 5. In the time domain, many identifiable peaks have been shifted by as much as 5 kyr. The coherence indicates that the record with inferred ages retains signals with periods greater than about 15 kyr, while the phase suggests these coherent signals remain nearly in phase. The results change very little when we look at other realizations of the tie point errors. However, when the age uncertainties are doubled, the coherence drops below the 95% confidence level at about 0.04 kyr^{-1}, increasing the minimum coherent period by 10 kyr.

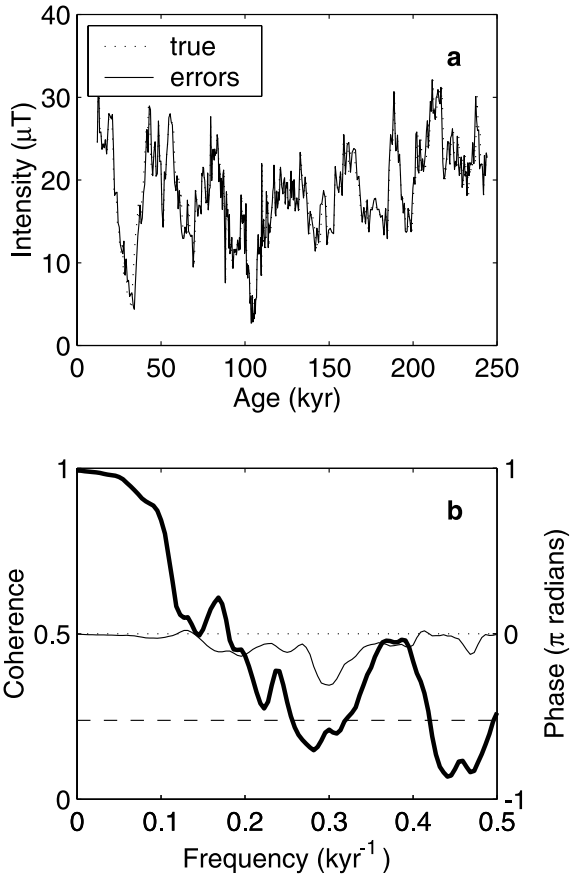

Fig. 6. Interpolation errors. $L=1$ cm, $a=0.5$. Same description as Fig. 4.

Table 1
Stage boundary ages, uncertainties [35] and applied errors (units of kyr)

Stage	Age	σ	Error
2	12.05	3.1	2.7
5	73.91	2.6	3.3
6	129.8	3.0	−4.8
7	189.6	2.3	−3.3
8	244.2	7.1	4.0

6.2. Interpolation errors

For a second experiment, we follow the methods of Section 3 and compare the spectral content of our reference record with that of a record contaminated solely with age errors due to variable accumulation rates on two lengthscales $L = 1$ cm and $L = 10$ cm.

For $L = 1$ cm, the time domain records (Fig. 6) show that peaks have been shifted by as much as 2 kyr. In the frequency domain, the results are considerably better than the previous case. The two records maintain significant coherence for periods greater than 5 kyr, while the phase remains stable and near zero.

The results for $L = 10$ cm (Fig. 7) are very different. In the time domain, peaks have been shifted by 5 kyr or more, while the longest coherent period has been reduced to about 15 kyr. We note the similarity of these results to those for event errors only.

6.3. Combined errors

Finally, we combine the two types of age errors and make a similar comparison. We choose interpolation errors with $L = 10$ cm because their magnitudes are similar to those due to event errors.

Table 2
List of symbols

a	parameter controlling the width of the distribution of X_i, and thus the magnitude of s_k^*
L	lengthscale of accumulation rate perturbations
M	$M+1$ steps in accumulation rate per section
$\mathcal{O}(\cdot)$	order of magnitude
RV	random variable
r_k	scaled sum of k RVs X_i
$t(z)$	inferred age at depth z
$\bar{s}$	constant background accumulation rate
s_k	perturbed accumulation rate between steps $k-1$ and k
s_k^*	relative perturbation in s_k
X_i	RVs uniformly distributed on $[1-a, 1+a]$
α	fractional distance between tie points
β	fractional distance between steps in accumulation rate
$\Delta\tau_k$	difference between adjacent actual ages τ_k and τ_{k-1}
σ_0, σ_M	standard deviation of errors in tie point ages
$\tau(z)$	actual age (random) at depth z

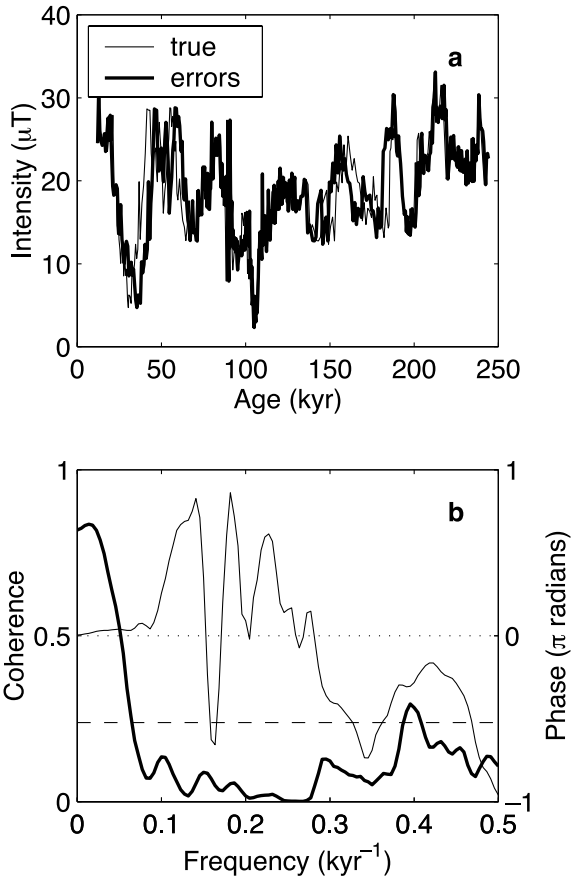

Fig. 7. Interpolation errors. $L = 10$ cm, $a = 0.5$. Same description as Fig. 4.

Fig. 8 demonstrates that the spectral content of the inferred record is better than those in the individual cases. We see peak displacements up to 5 kyr and coherent signals for periods greater than about 10 kyr. However, the signals become out of phase rapidly for slightly longer periods. These results suggest the possibility that a combination of age errors due to accumulation rate variations and errors in tie point ages can conspire to produce coherent, possibly out of phase, signals in a contaminated record.

7. Discussion and conclusions

We have developed a statistical model that quantifies potential age error in stratigraphic

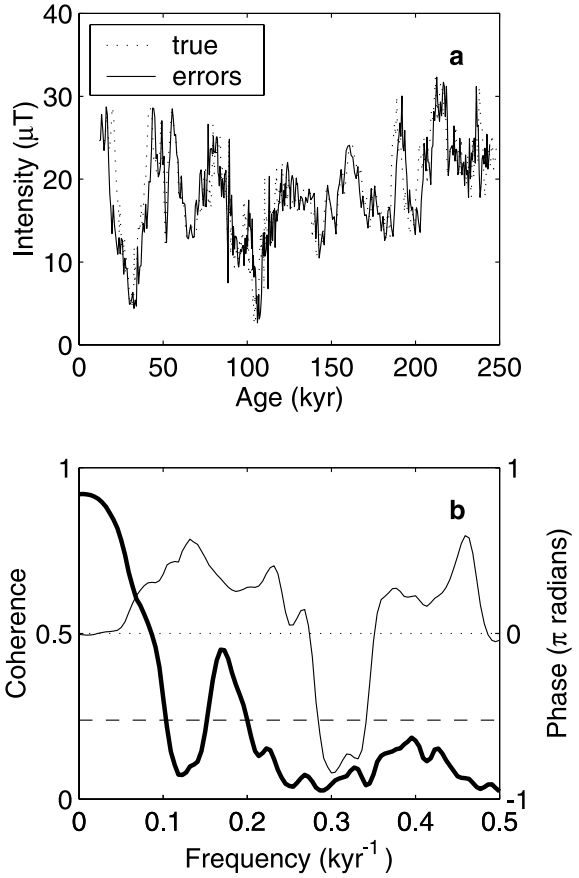

Fig. 8. Combined errors. $L = 10$ cm, $a = 0.5$. Same description as Fig. 4.

core records and have applied our methods to sedimentary paleomagnetism. Numerous related fields make similar assumptions when inferring dates for a record of some physical quantity. For example, oxygen isotope stratigraphy may be used to date geological or biological quantities [24]. In contrast, an alternative, such as the geomagnetic polarity timescale with linear interpolation of ages between reversals, has been used to date climate proxies in sedimentary cores [26]. Then, the errors in reversal ages (see [31]) are analogous to errors in our tie point ages and our analysis applies to the dating of climate proxy records.

The approach of Moore and Thompson [29] is similar to ours in that they quantify the effect of jitter on the spectral content of their signal. Their simplifying assumptions allow the reversal of samples and are limited to a specific family of spectral densities. Although our method can cause samples to switch places, the range of parameters useful for paleomagnetism makes this very unlikely. It might be possible to examine analytically spectral densities contaminated by our model, but likely only tractable for the simple case of event errors at two tie points. Huybers and Wunsch [30] propose a precise definition of jitter, but one that is not amenable to statistical analysis, except by observation. A particular difficulty in estimating age errors is the statistical characterization of variations in marine sediment accumulation. Huybers and Wunsch [30] introduce a promising spectral method that could help provide our analysis with a more realistic accumulation rate perturbation. Agrinier et al. [31] developed a statistical model that could be applied to sedimentary paleomagnetism. Rather than provide an explicit expression in terms of RVs for age errors, their method generates a suite of age realizations and a measure of the likelihood of each one.

We present a statistical analysis that is designed to model age errors in the simplest way possible under a variety of realistic stratigraphic conditions. We have kept the model simple in order to provide closed form expressions for the expected values (Eqs. 4 and 17) and variances of the age errors (Eqs. 5, 18 and 20). These expressions are essential to understanding the statistical properties of the age errors. Further, the standard deviations ($\sqrt{\text{variance}}$) may be used to estimate bounds on 1σ error bars for the inferred ages of a stratigraphic record. We note that this model is not intended to be a mathematical representation of physical processes such as deposition and magnetization acquisition. However, with different methods of calculating inferred age, it can be easily modified to account for samples of finite size and depth integrated acquisition of magnetization.

It is simple to quantify event errors for a record and we choose to model the tie point age uncertainties as zero-mean RVs. Alternatively, one might want to vary the tie point errors and examine their effects systematically. The statistical approach is favorable because it shows what is likely

(and sometimes what is unlikely) to occur, without the burden of examining an excessive number of model results or the myopia that results from compressing so many observations into a manageable form.

In the context of marine sediments, our goal has been to model age errors caused by variations in accumulation rate occurring independently of climate and glaciation effects. Some candidate physical mechanisms for these stochastic variations are: local disturbances in deposition rate; different rates of compaction over time; and episodic or periodic climate effects on decadal or centennial timescales. It is certain that accumulation rates vary significantly between stage boundaries. However, it is difficult to condense the often sparse data into simple statistical rules, especially when the data may not be capturing higher frequency variations. We have shown the model is capable of producing physically plausible accumulation rate variations (Fig. 3), but the paucity of relevant data puts a more comprehensive statistical assessment out of reach. We have neglected the problem of modeling erosion, which causes segments of paleomagnetic information to be missing from the measurements. Erosion, deterministic components and alternative stochastic variations in accumulation rates might be addressed by direct modeling of accumulation rate variations, then inferring age errors. We have found that to take this approach analytically, as we have done above, leads quickly to ungainly expressions that do not readily reveal illustrative quantities like the expected value or variance. In this case, one might resort to numerical simulations and so gain the freedom of specifying accumulation rates first, as in [31].

We have applied our model of age errors due to uncertain tie point ages (event errors) and due to accumulation rate variations between tie points (interpolation errors) in four experiments related to sedimentary paleomagnetism: each contribution separately and in combination. The event error at any distance between the tie points is itself likely to be of the same order as the tie point age uncertainties. Interpolation errors span a larger range depending on the lengthscale of the accumulation rate variations. For $L \sim \mathcal{O}(1)$ cm, interpolation errors are likely to be smaller than event errors, while larger L can yield age errors that are considerably greater than event errors. Our numerical experiments generate probable event errors of 3–7 kyr and up to 30 kyr interpolation errors (Table 1 and Fig. 4). The effects of each instability on the spectral content of records is severe. The combination of event and interpolation errors may produce significant coherence between the contaminated and clean signals. For a given set of uncertainties and many realizations, these are generally robust conclusions.

Acknowledgements

We gratefully acknowledge the following for their contributions to this effort. G.A. Glatzmaier supplied Gauss coefficients for our numerical experiments. J.J. Love, C.D. Charles, L. Tauxe, P. Huybers and A.W. Rempel participated in numerous discussions and contributed many worthwhile suggestions. We thank Peter M. Sadler and an anonymous reviewer who provided thoughtful critiques that led to significant improvements in our model and this paper. Funding was provided by NSF Grants EAR 01-12290, 00-00944 and IGPP LANL Grant #911.*[RV]*

References

[1] J. Imbrie, J.D. Hays, D.G. Martinson, A. McIntyre, A.C. Mix, J.J. Morley, N.G. Pisias, W.L. Prell, N.J. Shackleton, The orbital theory of Pleistocene climate: Support from a revised chronology of the marine $\delta^{18}O$ record, in: A. Berger, J. Imbrie, J. Hays, G. Kukla, B. Saltzman (Eds.), Milankovitch and Climate, Part I, Reidel, Boston, 1984, pp. 269–305.

[2] J. Imbrie, A. McIntyre, A.C. Mix, Oceanic response to orbital forcing in the late Quaternary: Observational and experimental strategies, in: A. Berger, S.H. Schneider, J.-C. Duplessy (Eds.), Climate and Geosciences: A Challenge for Science and Society in the 21st Century, Kluwer Academic Publishers, Boston, 1989, pp. 121–164.

[3] S.J. Johnsen, H.B. Clausen, W. Dansgaard, N.S. Gundestrup, C.U. Hammer, U. Anderson, K.K. Anderson, C.S. Hvidberg, D. Dahl-Jensen, J.P. Steffensen, H. Shoji, Á.E. Sveinbjörnsdóttir, J. White, J. Jouzel, D. Fisher, The $\delta^{18}O$ record along the Greenland Ice Core Project deep ice

core and the problem of possible Eemian climatic instability, J. Geophys. Res. 102 (1997) 26397–26410.
[4] D. Lal, Theoretically expected variations in the terrestrial cosmic-ray production rates of isotopes, Soc. Ital. Fisc. Bologna 95 (1988) 216–233.
[5] F. Yiou, G.M. Raisbeck, S. Baumgartner, J. Beer, C. Hammer, S. Johnsen, J. Jouzel, P.W. Kubik, J. Lestringuez, M. Stiévenard, M. Suter, P. Yiou, Beryllium 10 in the Greenland Ice Core Project ice core at Summit, Greenland, J. Geophys. Res. 102 (1997) 26783–26794.
[6] M. Frank, B. Schwarz, S. Baumann, P.W. Kubik, M. Suter, A. Mangini, A 200 kyr record of cosmogenic radionuclide production rate and geomagnetic field intensity from ^{10}Be in globally stacked deep-sea sediments, Earth Planet. Sci. Lett. 149 (1997) 121–129.
[7] S. Baumgartner, J. Beer, J. Masarik, G. Wagner, L. Meynadier, H.-A. Synal, Geomagnetic modulation of the ^{36}Cl flux in the GRIP ice core, Greenland, Science 279 (1998) 1330–1332.
[8] J.C. Moore, E.W. Wolff, H.B. Clausen, C.U. Hammer, The chemical basis for the electrical stratigraphy of ice, J. Geophys. Res. 97 (1992) 1887–1896.
[9] K. Taylor, R. Alley, J. Fiacco, P. Grootes, G. Lamorey, P. Mayewski, M.J. Spencer, Ice-core dating and chemistry by direct current electrical conductivity, J. Glaciol. 38 (1992) 325–332.
[10] K.C. Taylor, R.B. Alley, G.W. Lamorey, P. Mayewski, Electrical measurements on the Greenland Ice Sheet Project 2, J. Geophys. Res. 102 (1997) 26511–26517.
[11] L. Tauxe, Sedimentary records of relative paleointensity of the geomagnetic field: Theory and practice, Rev. Geophys. 31 (1993) 319–354.
[12] Y. Guyodo, J.-P. Valet, Relative variations in geomagnetic intensity from sedimentary cores: The past 200,000 years, Earth Planet. Sci. Lett. 143 (1996) 23–36.
[13] D.A. Meese, A.J. Gow, P. Grootes, P.A. Mayewski, M. Ram, M. Stuiver, K.C. Taylor, E.D. Waddington, G.A. Zielinski, The accumulation record from the GISP2 core as an indicator of climate change throughout the Holocene, Science 266 (1994) 1680–1682.
[14] L.C. Peterson, J.T. Overpeck, N.G. Kipp, J. Imbrie, A high-resolution late Quaternary upwelling record from the anoxic Cariaco basin, Venezuala, Paleoceanography 6 (1991) 99–119.
[15] K.C. Taylor, C.U. Hammer, R.B. Alley, H.B. Clausen, D. Dahl-Jensen, A.J. Gow, N.S. Gundestrup, J. Kipfstul, J.C. Moore, E.D. Waddington, Electrical conductivity measurements from the GISP2 and GRIP Greenland ice cores, Nature 366 (1993) 549–552.
[16] P.M. Grootes, M. Stuiver, J.W.C. White, S. Johnsen, J. Jouzel, Comparison of oxygen isotope records from the GISP2 and GRIP Greenland ice cores, Nature 366 (1993) 552–554.
[17] A.J. Gow, T. Williamson, Rheological implications of the internal structure and crystal fabrics of the West Antarctic ice sheet as revealed by deep core drilling at Byrd station, Geol. Soc. Am. Bull. 87 (1975) 1665–1677.
[18] T. Thorsteinsson, J. Kipfstul, H. Eicken, S.J. Johnsen, K. Fuhrer, Crystal size variations in Eemian-age ice from the GRIP ice core, Central Greenland, Earth Planet. Sci. Lett. 131 (1995) 381–394.
[19] I. Hadjas, S.D. Ivy, J. Beer, G. Bonani, D. Imboden, A.F. Lotter, M. Sturm, M. Suter, AMS radiocarbon dating and varve chronology of Lake Soppensee: 6000 to 12000 years BP, Clim. Dyn. 9 (1993) 107–116.
[20] I. Hadjas, B. Zolitschka, S.D. Ivy-Ochs, J. Beer, G. Bonani, S.A.G. Leroy, J.W. Negendank, M. Ramrath, M. Suter, AMS radiocarbon dating of annually laminated sediments from Lake Holzmaar, Germany, Quat. Sci. Rev. 14 (1995) 137–143.
[21] E. Bard, B. Hamelin, R.G. Fairbanks, A. Zindler, Calibration of the ^{14}C timescale over the past 30,000 years using mass spectrometric U-Th ages from Barbados corals, Nature 345 (1990) 405–410.
[22] M. Stuiver, P.J. Reimer, E. Bard, J.W. Beck, G.S. Burr, K.A. Hughen, B. Kromer, G. McCormac, J. van der Plicht, M. Spurk, INTCAL98 radiocarbon age calibration, 24,000-0 cal BP, Radiocarbon 40 (1998) 1041–1083.
[23] R.L. Edwards, J.H. Chen, G.J. Wasserburg, ^{238}U-^{234}U-^{230}Th-^{232}Th systematics and the precise measurement of time over the past 500,000 years, Earth Planet. Sci. Lett. 81 (1987) 175–192.
[24] U. Brathauer, A. Abelmann, R. Gersonde, H.-S. Niebler, D.K. Fütterer, Calibration of *Cycladophora davisiana* events versus oxygen isotope stratigraphy in the subantarctic ocean – a stratigraphic tool for carbonate-poor Quaternary sediments, Mar. Geol. 175 (2001) 167–181.
[25] K. Gronvold, N. Oskarsson, S.J. Johnsen, H.B. Clausen, C.U. Hammer, G. Bond, E. Bard, Ash layers from iceland in the Greenland GRIP ice core correlated with oceanic and land sediments, Earth Planet. Sci. Lett. 135 (1995) 149–155.
[26] K. Kashiwaya, S. Ochiai, H. Sakai, T. Kawai, Orbit-related long-term climate cycles revealed in a 12-Myr continental record from Lake Baikal, Nature 410 (2001) 71–74.
[27] S.J. Johnsen, W. Dansgaard, On flow model dating of stable isotope records from Greenland ice cores, in: E. Bard, W.S. Broecker (Eds.), NATO ASI Series Vol. I 2, The Last Deglaciation: Absolute and Radiocarbon Chronologies, Springer, Berlin, 1992, pp. 13–24.
[28] T. Blunier, J. Chappellaz, J. Schwander, A. Dällenbach, B. Stauffer, T.F. Stocker, D. Reynaud, J. Jouzel, H.B. Clausen, C.U. Hammer, S.J. Johnsen, Asynchrony of Antarctic and Greenland climate change during the last glacial period, Nature 394 (1998) 739–743.
[29] M.I. Moore, P.J. Thomson, Impact of jittered sampling on conventional spectral estimates, J. Geophys. Res. 96 (1991) 18519–18526.
[30] P. Huybers, C. Wunsch, Re-evaluating the orbital theory of Pleistocene climate, EOS Trans. AGU Fall Meet. Suppl. 82 (2001) Abstr. U12A-0002.
[31] P. Agrinier, Y. Gallet, E. Lewin, On the age calibration of

the geomagnetic polarity timescale, Geophys. J. Int. 137 (1999) 81–90.
[32] C. Laj, C. Kissel, A. Mazaud, J.E.T. Channell, J. Beer, North Atlantic palaeointensity stack since 75 ka (NAPIS-75) and the duration of the Laschamp event, Philos. Trans. R. Soc. Lond. 358 (2000) 1009–1025.
[33] Y. Guyodo, J.-P. Valet, Global changes in intensity of the Earth's magnetic field during the past 800 kyr, Nature 399 (1999) 249–252.
[34] L. Tauxe, G. Wu, Normalized remanence in sediments of the western equatorial Pacific: Relative paleointensity of the geomagnetic field?, J. Geophys. Res. 95 (1990) 12337–12350.
[35] D.G. Martinson, N.G. Pisias, J.D. Hays, J. Imbrie, T.C. Moore, N.J. Shackleton, Age dating and orbital theory of ice ages: Development of a high resolution 0 to 300,000-year chronostratigraphy, Quat. Res. 27 (1987) 1–29.
[36] E. Tric, J.-P. Valet, M. Paterne, L. Labeyrie, F. Guichard, L. Tauxe, M. Fontugne, Paleointensity of the geomagnetic field during the last 80,000 years, J. Geophys. Res. 97 (1992) 9337–9351.
[37] T. Yamazaki, N. Ioka, Long-term secular variation of the geomagnetic field during the last 200 k.y. recorded in sediment cores from the western equatorial Pacific, Earth Planet. Sci. Lett. 128 (1994) 527–544.
[38] B. Lehman, C. Laj, C. Kissel, A. Mazaud, M. Paterne, L. Labeyrie, Relative changes of the geomagnetic field intensity during the last 280 kyear from piston cores in the acores area, Phys. Earth Planet. Inter. 93 (1996) 269–284.
[39] D.R. Bhattacharya, E.C. Waymire, Stochastic Processes with Applications, Wiley, New York, 1990, 35 pp.
[40] A. Jackson, A.R.T. Jonkers, M.R. Walker, Four centuries of geomagnetic secular variation from historical observations, Philos. Trans. R. Soc. Lond. 358 (2000) 957–990.
[41] J.A. Rice, Mathematical Statistics and Data Analysis, Wadsworth and Brooks, Belmont, 1988, 142 pp.
[42] J.S. Stoner, J.E.T. Channell, C. Hillaire-Marcel, A 200 kyr geomagnetic chronostratigraphy for the Labrador Sea: Indirect correlation of the sediment record to SPECMAP, Earth Planet. Sci. Lett. 159 (1998) 165–181.
[43] G.A. Glatzmaier, R.S. Coe, L. Hongre, P.H. Roberts, The role of Earth's mantle in controlling the frequency of geomagnetic reversals, Nature 401 (1999) 885–890.
[44] D.G. McMillan, C.G. Constable, R.L. Parker, G.A. Glatzmaier, A statistical analysis of magnetic fields from some geodynamo simulations, Geochem. Geophys. Geosyst. 2 (2001) paper number 2000GC000130.
[45] N. Teanby, D. Gubbins, The effects of aliasing and lock-in processes on palaeosecular variation records from sediments, Geophys. J. Int. 142 (2000) 563–570.